

A nonplanar Peierls-Nabarro model and its applications to dislocation cross-slip

Gang Lu,¹ Vasily V. Bulatov,² and Nicholas Kioussis³

¹*Department of Physics and Division of Engineering and Applied Science,
Harvard University, Cambridge, MA 02138*

²*Lawrence Livermore National Laboratory, Livermore, CA 94550*

³*Department of Physics, California State University Northridge, Northridge, CA 91330*

Abstract

A novel semidiscrete Peierls-Nabarro model is introduced which can be used to study dislocation spreading at more than one slip planes, such as dislocation cross-slip and junctions. The strength of the model, when combined with *ab initio* calculations for the energetics, is that it produces essentially an atomistic simulation for dislocation core properties without suffering from the uncertainties associated with empirical potentials. Therefore, this method is particularly useful in providing insight into alloy design when empirical potentials are not available or not reliable for such multi-element systems. As an example, we study dislocation cross-slip and constriction process in two contrasting fcc metals, Al and Ag. We find that the screw dislocation in Al can cross-slip spontaneously in contrast with that in Ag, where the screw dislocation splits into two partials, which cannot cross-slip without first being constricted. The response of the dislocation to an external stress is examined in detail. The dislocation constriction energy and the critical stress for cross-slip are determined, and from the latter, we estimate the cross-slip energy barrier for straight screw dislocations.

The past decades have witnessed a growing interest towards a quantitative understanding of deformation and strength of materials and, in particular, the effect of impurities and alloying elements on dislocation properties. While continuum elasticity theory describes well the long-range elastic strain of a dislocation for length scales beyond a few lattice spacings, it breaks down near the singularity in the region surrounding the dislocation center, known as the dislocation core. There has been a great deal of interest in describing accurately the dislocation core structure on an atomic scale because of its important role in many phenomena of crystal plasticity [1, 2]. The core properties control, for instance, the mobility of dislocations, which accounts for the intrinsic ductility or brittleness of solids. The core is also responsible for the interaction of dislocations at close distances, which is relevant to plastic deformation. For example, by integrating the local rules derived from atomistic simulations of core interactions into dislocation-dynamics simulations, a connection between micro-to-meso scales can be established to study dislocation reactions and crystal plasticity [3].

Cross-slip, the process by which a screw dislocation moves from one glide plane to another, is ubiquitous in plastic deformation of materials. For example, cross-slip is considered to be responsible for the onset of stage III in the stress-strain work-hardening curves. Furthermore, cross-slip can result in the formation of glide plane obstacles (sessile segments) in hcp metals and in L1₂-, B2- and L1₀- based intermetallic alloys, responsible for the anomalous high-temperature yield stress peak. However, theoretical studies of alloying and impurity effects on dislocation cross-slip have proved to be particularly difficult because one has to deal with both long-ranged elastic interactions (between dislocation segments) and short-ranged atomic interactions (due to the constriction process) that are inherent in a cross-slip process.

There are currently two theoretical approaches to study cross-slip. One is based on the line tension approximation which completely ignores atomic interactions, therefore it is not reliable [4, 5]. The other approach is direct atomistic simulations employing empirical potentials [6, 7]. Although the second approach is quite powerful in determining cross-slip transition paths and estimating the corresponding activation energy barriers, it is time-consuming and, more importantly, it critically depends on the accuracy and availability of the empirical potentials employed in the simulations. For example, reliable interatomic potentials usually are not available for multi-elements materials. As a consequence, the possible hardening mechanisms due to alloying for most materials are still uncertain, and

the design of new materials based on favorable cross-slip properties lacks guidance. Thus, the understanding at an atomic level of the chemistry effect on the dislocation core properties and cross-slip mechanisms is of great importance in predicting and controlling plastic deformation in structural materials, since the deformation behavior is often associated with the presence of substitutional or interstitial alloying elements. The ultimate goal of theoretical studies is then to use this information to direct alloying design for new materials with desired mechanical properties by tailoring the dislocation properties - in close collaboration with experimental efforts.

In this paper, we introduce a novel model based on the Peierls-Nabarro (P-N) framework which allows the study of dislocation cross-slip employing *ab initio* calculations. In fact, there has been a resurgence of interest recently in applying the simple and tractable P-N model to study dislocation core structure and mobility in conjunction with *ab initio* γ -surface calculations [8, 9, 10, 11, 12, 13]. This approach represents a combination of an atomistic (*ab initio*) treatment of the interactions across the slip plane and an elastic treatment of the continua on either side of the slip plane. Therefore, this approach is particularly useful for studying the interaction of impurities with dislocations when empirical potentials are either not available or not reliable to deal with such multi-element systems. Furthermore, it allows to study general trends in dislocation core properties and to correlate them with specific features of the underlying electronic structure. However, to date, all models based on the P-N framework are applicable only to a single slip plane while the important cross-slip process requires at least two active intersecting slip planes, i.e., the primary and cross-slip planes. In this work the semidiscrete variational P-N model[10, 12, 13] is extended so as to take into account two intersecting slip planes. We shall apply this new model to study the dislocation constriction and cross-slip process in two fcc metals, Al and Ag, exhibiting different deformation properties. We are particularly interested in the evolution of the dislocation core structure under external stress and the interplay between the applied stress and the cross-slip process.

We begin by developing an appropriate energy functional for the Peierls dislocation at two intersecting slip planes. To facilitate presentation, we adopt the following conventions: In Fig. 1, a screw dislocation placed at the intersection of the primary (plane I) and cross-slip plane (plane II) is allowed to spread into the two planes simultaneously. The X (X') axis represents the glide direction of the dislocation at the plane I (II). For an fcc lattice, the two

slip planes are (111) and ($\bar{1}11$), forming an angle $\theta \approx 71^\circ$. The dislocation line is along the $[10\bar{1}]$ (Z axis) direction and L represents the outer radius of the dislocation beyond which the configuration independent elastic energy is ignored.[12] In the spirit of the P-N model, the dislocation is represented as a continuous distribution of infinitesimal dislocations with densities of $\rho^I(x)$ and $\rho^{II}(x')$ on the primary and cross-slip planes, respectively, where, x and x' are the coordinates of the atomic rows at the two planes. Following the semidiscrete Peierls framework developed earlier [10, 12], the total energy of the dislocation is

$$U_{tot} = U_I + U_{II} + \tilde{U}. \quad (1)$$

Here, U_I and U_{II} are the energies associated with the dislocation spread on planes I and II, respectively, and \tilde{U} represents the elastic interaction energy between the dislocation densities on planes I and II. The expressions for U_I and U_{II} are identical to that given earlier for the single glide plane case [10, 12], while the new term \tilde{U} can be derived from Nabarro's equation for general parallel dislocations [14],

$$\begin{aligned} U_{I(II)} &= \sum_{i,j} \frac{1}{2} \chi_{ij} \{ K_e [\rho_1^{I(II)}(i) \rho_1^{I(II)}(j) + \rho_2^{I(II)}(i) \rho_2^{I(II)}(j)] + K_s \rho_3^{I(II)}(i) \rho_3^{I(II)}(j) \} \\ &\quad + \sum_i \Delta x \gamma_3 (f_1^{I(II)}(i), f_2^{I(II)}(i), f_3^{I(II)}(i)) - \sum_{i,l} \frac{x(i)^2 - x(i-1)^2}{2} \rho_l^{I(II)}(i) \tau_l^{I(II)} + K b^2 \ln L, \\ \tilde{U} &= - \sum_{i,j} K_s \rho_3^I(i) \rho_3^P(j) A_{ij} - \sum_{i,j} K_e [\rho_1^I(i) \rho_1^P(j) + \rho_2^I(i) \rho_2^P(j)] A_{ij} \\ &\quad - \sum_{i,j} K_e [\rho_2^I(i) \rho_2^P(j) B_{ij} + \rho_1^I(i) \rho_1^P(j) C_{ij} - \rho_2^I(i) \rho_1^P(j) D_{ij} - \rho_1^I(i) \rho_2^P(j) D_{ij}]. \end{aligned}$$

Here, $f_1^{I(II)}(i)$, $f_2^{I(II)}(i)$ and $f_3^{I(II)}(i)$ represent the edge, vertical and screw component of the general dislocation displacement at the i -th nodal point in plane I(II), respectively, while the corresponding component of dislocation density in plane I(II) is defined as $\rho^{I(II)}(i) = (f^{I(II)}(i) - f^{I(II)}(i-1)) / (x(i) - x(i-1))$. The projected dislocation density $\rho^P(i)$ is the projection of the density $\rho^{II}(i)$ from plane II onto plane I in order to deal with the non-parallel components of the displacement. The γ -surface, γ_3 , which in general includes shear-tension coupling can be determined from *ab initio* calculations. $\tau_l^{I(II)}$ is the external stress component interacting with the corresponding dislocation densities, $\rho_l^{I(II)}(i)$ ($l = 1,2,3$). This term represents the contribution to the total energy from the elastic work done by the applied stress [10, 12]. The response of a dislocation to an applied stress is achieved by the minimization of the energy functional with respect to $\rho_l^{I(II)}(i)$ at the given value of

$\tau_l^{I(II)}$. The dislocation core energy is defined as the configuration-dependent part of the total energy, which includes the density-dependent part of the elastic energy and the entire misfit energy, in the absence of stress [12]. K_e and K_s are the edge and screw components of the general prelogarithmic elastic energy factor K [10, 12], while χ_{ij} , A_{ij} , B_{ij} , C_{ij} and D_{ij} are double-integral kernels defined by

$$\begin{aligned}\chi_{ij} &= \int_{x_{j-1}}^{x_j} \int_{x_{i-1}}^{x_i} \ln|x-x'| dx dx', \\ A_{ij} &= \int_{x'_{j-1}}^{x'_j} \int_{x_{i-1}}^{x_i} \frac{1}{2} \ln(x_0^2 + y_0^2) dx dx', \\ B_{ij} &= \int_{x'_{j-1}}^{x'_j} \int_{x_{i-1}}^{x_i} \ln \frac{x_0^2}{x_0^2 + y_0^2} dx dx', \\ C_{ij} &= \int_{x'_{j-1}}^{x'_j} \int_{x_{i-1}}^{x_i} \ln \frac{y_0^2}{x_0^2 + y_0^2} dx dx', \\ D_{ij} &= \int_{x'_{j-1}}^{x'_j} \int_{x_{i-1}}^{x_i} \ln \frac{x_0 y_0}{x_0^2 + y_0^2} dx dx',\end{aligned}$$

where $x_0 = L - x + x' \cos \theta$, and $y_0 = -x' \sin \theta$. The equilibrium structure of the dislocation is determined by minimizing the total dislocation energy functional energy with respect to the dislocation density.

In order to compare and understand the different cross-slip behavior in Al and Ag, we have carried out *ab initio* calculations for their γ -surfaces. In both calculations, we used a supercell containing six layers of atoms in the [111] direction. The *ab initio* calculations are based on the pseudopotential plane-wave method [15] within the local density approximation. Owing to the planar nature of the dislocation core structure in fcc metals, we disregard in the γ -surface calculations the displacement perpendicular to the slip planes and consider partially the shear-tension coupling by performing volume relaxation along the [111] direction. The complete γ -surface for Al and Ag is shown in Fig. 2(a) and 2(b) respectively. The most striking difference between the two γ -surfaces is the large difference in intrinsic stacking fault energy, which is 165 mJ/m² for Al and 14 mJ/m² for Ag. This dramatic difference in γ -surface gives rise to very different dislocation core structures and cross-slip behavior that we are going to explore. The *ab initio* calculated Burgers vector, b , of a perfect 1/2[101]

dislocation in Al and Ag is 2.85 and 2.83 Å, respectively.

The model calculation is set up by introducing a screw dislocation at the intersection of the two slip planes without applying external stress to the system at first. The initial configuration of the dislocation is specified by a step function for the screw displacement $f_3^I(x) = 0$ for $x < L$ and $f_3^I(x) = b$ for $x \geq L$. All other displacement components including those on the cross-slip plane are set initially to zero. This corresponds to a pure screw dislocation with a zero width “spread” on the primary plane. We then relax the dislocation structure according to the energy functional. The results of the dislocation density $\rho(x)$ in the primary and cross-slip planes for Al and Ag are presented in Figs. 3(a) and 3(b), respectively. The screw dislocation in Al which starts out at the primary plane spontaneously spreads into the cross-slip plane, as the density peak at the cross-slip plane indicates. As expected, the edge component of the density is zero at the cross-slip plane because only the screw displacement can cross-slip. On the other hand, the screw dislocation in Ag dissociates into two partials, separated by $7.8 b$ (≈ 22 Å), in excellent agreement with the experimental value of 20 Å in TEM measurements [17]. The left (right) partial has a positive (negative) edge component of the Burgers vector represented by the positive (negative) density. The integral of the edge density over all atomic sites is zero, corresponding to a pure screw dislocation. These partial dislocations cannot cross-slip, as the arrows in Fig. 3(a) indicate, without first annihilating their edge components, and the dislocation density on the cross-slip plane is essentially zero. Apparently, the lack of obvious dissociation in Al stems from the fact that Al has a much higher intrinsic stacking fault energy than Ag. The absence of obvious dissociation into partials in Al is also consistent with experiment [18].

Next we apply an external Escaig stress to the dislocations and examine the evolution of the dislocation core structure under stress with the emphasis on the effect of stress on the dislocation cross-slip. The Escaig stress, defined as the edge component of the diagonal stress tensor, interacts only with the edge displacement of a dislocation, extending or shrinking its stacking fault width depending on the sign of the stress. We apply the Escaig stress only on the dislocation at the primary plane, and the stress components projected on the cross-slip plane are removed. The evolution of the dislocation core structure in Ag, represented by its displacement density distribution, is presented in Fig. 4 as the Escaig stress is varied. Upon application of positive (stretching) stress of $\tau_1^I = 0.32$ GPa, the separation of the partials rises rapidly from $7.8 b$ (equilibrium separation in the absence of applied stress) to $12 b$ (Fig.

4(a)). In Fig. 4(a) we show only the density at the primary plane, as the density at the cross-slip plane is essentially zero. For stress higher than 0.32 GPa, the partials move to the two ends of the simulation box and the lattice breaks down. To activate cross-slip, however, one needs to apply a negative (compressive) Escaig stress to the dislocation in order to annihilate the edge components of the partials' displacement, known as a constriction process. Upon application of negative stress, the partials move towards each other and reduce the width of the stacking fault. During this process, the edge components of the displacement from the two partials annihilate each other at the primary plane while the screw component is being built up at both planes. One example of such structure is shown in Fig. 4(b). The left and right density peaks represent the original two partial dislocations, while the third peak at the center corresponds to the build-up of the screw density from the overlapping partials. Interestingly, the screw component of the dislocation density at the cross-slip plane is also accumulating, indicating the inception of the cross-slip process. However, further increasing the negative Escaig stress does not yield smaller separation between the partials. We find that the lower limit for the partials separation in Ag is $1.7 b$, which is in agreement with the atomistic simulation result for Cu, reporting a corresponding value of $1.6 b$ [19]. In other words, no complete constriction can be achieved for a straight dislocation. The critical configuration in which the constriction is most developed is shown in Fig. 4(c). In this case, three partial dislocations with the same amount of screw component of the Burgers vector are formed. The cross-slipped screw dislocation density is about one third of the remaining screw density at the primary plane. In order to complete the cross-slip, either thermal fluctuations or other type of external stress have to be present. This is because the remaining edge component of the partials interacts with the Escaig stress, and as a result the partials exchange signs and move away from each other. For example, as shown in Fig. 4(d), the left partial now acquires a negative edge density and the right partial a positive edge density. Associated with the inversion of the edge component of the density for the partials, a run-on stacking fault is formed between them, with an energy of about 1.0 J/m^2 . The run-on stacking fault is the most unstable stacking fault in an fcc lattice, with atoms from the neighboring (111) planes sitting right on top of each other. The distance between the two partials is more than $10 b$. It is interesting to note that in the wake of the (partial) constriction process, a pure screw dislocation segment is formed at the intersection of the two planes, with an appreciable amount of cross-slip.

Next we examine the situation of Al. We first apply positive Escaig stress to the complete screw dislocation. We find that the screw dislocation remains unsplit until the stress reaches the threshold value of 0.96 GPa, required to separate the overlapping partials. The dislocation core structure corresponding to such a stress-driven dissociation is shown in Fig. 5(a). We find that the screw density component at the cross-slip plane is only reduced by a few percent due to the small splitting, leaving the density at the cross-slip plane approximately equal to that in the primary plane. Increasing the positive stress will further separate the partials and reduce cross-slip. The maximum positive Escaig stress, however, that the dislocation can sustain is 1.92 GPa (Fig. 5(b)). In this configuration, the partials are separated by $5 b$. The central peak in the screw density plot corresponding to the original complete dislocation is reduced significantly, and the cross-slipped screw density amounts to only $1/3$ of the screw density at the primary plane. Therefore, the application of positive Escaig stress in Al corresponds to an “inverse cross-slip” process that transfers displacement from the “cross-slip” plane to the “primary plane”. Interestingly, applying negative Escaig stress to the dislocation has no effect on the dislocation splitting or core width. The dislocation remains unsplit all the way until the stress is great enough to break down the lattice. Finally, it is important to point out that for all cases studied here in Al and Ag, upon removal of the applied external stress, the dislocation returns spontaneously to its equilibrium configuration.

We have also estimated the critical energetics that are relevant to cross-slip. For example, we calculated the constriction energy, defined as the difference in dislocation core energy between the normal and constricted states. By approximating the state with $1.7 b$ separation between the partials as the constricted state, we were able to estimate the constriction energy for Ag to be $0.14 \text{ eV}/b$. A similar approach has been used to evaluate the constriction energy for a screw dislocation in Cu based on atomistic simulations, reporting a value of $0.17 \text{ eV}/b$, which is in a good agreement with our model calculations [19]. Obviously, the constriction energy for Al is zero because its normal state is fully constricted. We have also calculated the critical stress for cross-slip, which is defined as the glide stress in the cross-slip plane to move a partially constricted dislocation from the primary to the cross-slip plane [19]. We find that the critical stress for cross-slip in Ag is 1.68 GPa, compared to 0.32 GPa in Al. Finally, we estimated the cross-slip energy barrier, which in the context of our calculations, is defined as the difference in dislocation core energy before and after cross-slip takes place

under the application of the above mentioned critical stress for cross-slip. In other words, we calculate the core energy difference for the dislocation between its normal state and the state that the dislocation just starts to cross-slip under the critical cross-slip stress. We find that the cross-slip energy barrier in Ag is 0.14 eV/ b , much larger than that of 0.05 eV/ b in Al. One needs to be cautious when comparing our results for the cross-slip energy barrier directly with experiment, since the dislocations are assumed to be straight in our current implementation of the Peierls-Nabarro model. However, it is possible to extend the present formalism to deal with an arbitrarily curved dislocation where a more realistic cross-slip energy barrier can be obtained. Nevertheless, the present model is still capable to provide reliable energetics for straight dislocations.

In summary, we have presented a novel model based on the semidiscrete Peierls-Nabarro framework that allows the study of dislocation cross-slip and constriction. The γ -surface entering the model is determined from *ab initio* calculations which provide reliable atomic interactions across the slip plane. We find that the screw dislocation in Al can spontaneously spread into the cross-slip plane, while in Ag it dissociates into partials and can not cross-slip. We have also examined in detail the response of the dislocation core structure to an external Escaig stress and the effect of negative Escaig stress on the constriction of the Shockley partials. We find that one can not achieve 100% constriction for the case of straight partial dislocations considered in this work. By computing the dislocation core energy under stress we estimate the dislocation constriction energy for Al and Ag. The calculated values of the critical stress and the energy barrier for dislocation cross-slip demonstrate that dislocation cross-slip is much easier in Al than in Ag. Since our *ab initio* based model is much more expedient than direct *ab initio* atomistic simulations, it can serve as a powerful and efficient tool for alloy design, where the goal is to select the “right” elements with the “right” alloy composition to tailor desired mechanical, and in particular, dislocation properties, such as cross-slip properties.

Acknowledgments

Two of us (G.L. and N.K.) acknowledge the support from Grant No. DAAD19-00-1-0049 through the U.S. Army Research Office. G.L. was also supported by Grant No. F49620-99-

1-0272 through the U.S. Air Force Office for Scientific Research.

- [1] M. S. Duesbery, and G. Y. Richardson, *CRC Crit. Rev. Solid State Mater. Sci.*, **17**, 1 (1991).
- [2] V. Vitek, *Progress in Materials Science*, **36**, 1 (1992).
- [3] V. Bulatov, F. F. Abraham, L. Kubin, B. Devincere and S. Yip, *Nature*, **391**, 669 (1998).
- [4] J. Friedel, in *Dislocations and Mechanical properties of Crystals*, edited by J.C. Fisher (Wiley, New York, 1957).
- [5] B. Escaig, in *Dislocation Dynamics*, edited by A.R. Rosenfeld *et al.* (McGraw-Hill, New York, 1968).
- [6] T. Rasmussen, K.W. Jacobsen, T. Leffers, O.B. Pederson, S.G. Srinivasan, and H. Jónsson, *Phys. Rev. Lett.* **79**, 3676 (1997).
- [7] S. Rao, T.A. Parthasarathy, and C. Woodward, *Philos. Mag. A* **79**, 1167 (1999).
- [8] B. Joós, Q. Ren and M.S. Duesbery, *Phys. Rev. B* **50**, 5890 (1994).
- [9] Y.M. Juan and E. Kaxiras, *Philos. Mag. A* **74**, 1367 (1996).
- [10] V. V. Bulatov and E. Kaxiras, *Phys. Rev. Lett.* **78**, 4221 (1997).
- [11] J. Hartford, B. von Sydow, G. Wahnström, and B.I. Lundqvist, *Phys. Rev. B* **58**, 2487 (1998).
- [12] G. Lu, N. Kioussis, V. V. Bulatov, and E. Kaxiras, *Phys. Rev. B* **62**, 3099 (2000); *Philos. Mag. Lett.* **80**, 675 (2000).
- [13] G. Lu, Q. Zhang, N. Kioussis, and E. Kaxiras, *Phys. Rev. Lett.* **87**, 095501 (2001).
- [14] F.R.N. Nabarro, *Adv. Phys.*, **1**, 269 (1952).
- [15] M.C. Payne, M.P. Teter, D.C. Allan, T.A. Arias and J.D. Joannopoulos, *Rev. Mod. Phys.*, **64**, 1045 (1992).
- [16] J.P. Hirth and J. Lothe, *Theory of Dislocations*, 2nd ed. (Wiley, New York, 1992).
- [17] D.J.H. Cockayne, M.L.Jenkins and I.L.F. Ray, *Philos. Mag.* **24**, 1383 (1971).
- [18] M. S. Duesbery, *Dislocations in Solids*, edited by F.R.N. Nabarro (North-Holland, Amsterdam, 1989), Vol. 8, p.67.
- [19] M.S. Duesbery, *Modelling Simul. Mater. Sci. Eng.* **6**, 35 (1998).

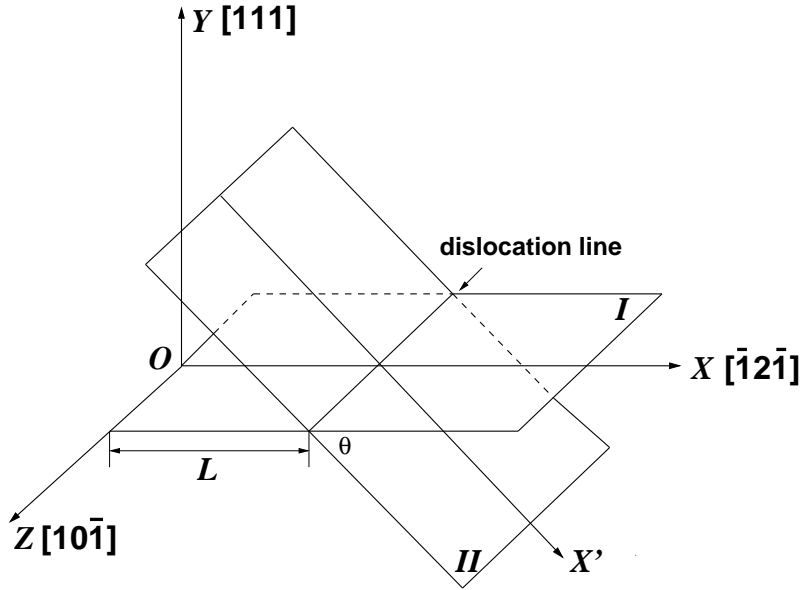


FIG. 1: Cartesian set of coordinates showing the directions relevant to the screw dislocation located at the intersection of the two slip planes. Plane I (II) denotes the primary (cross-slip) plane.

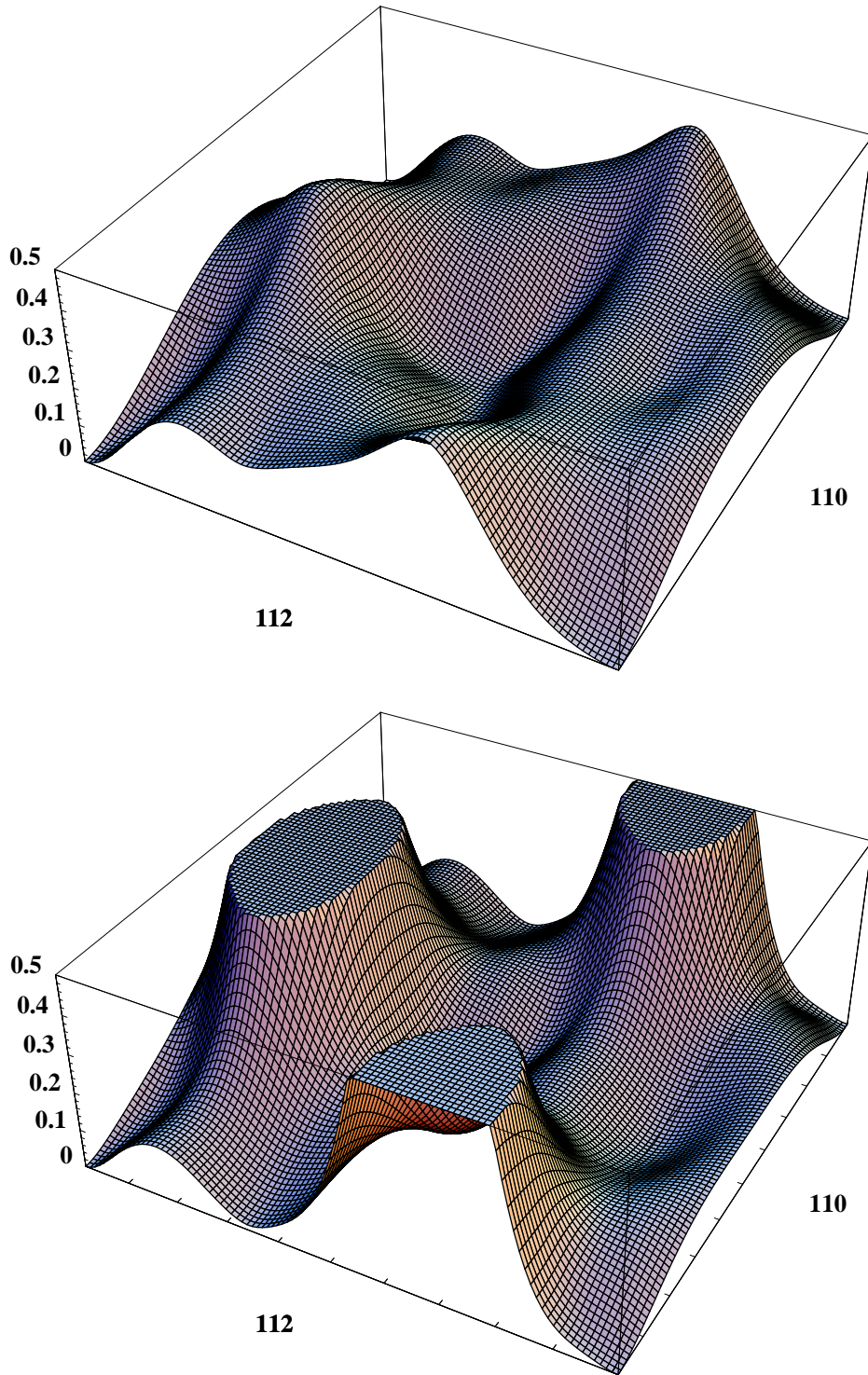


FIG. 2: The γ -surfaces (J/m^2) for displacements along a (111) plane for (a) Al and (b) Ag . The corners of the plane and its center correspond to identical equilibrium configurations, i.e., the ideal lattice. The two energy surfaces are displayed in exactly the same perspective and on the same energy scale to facilitate comparison of important features.

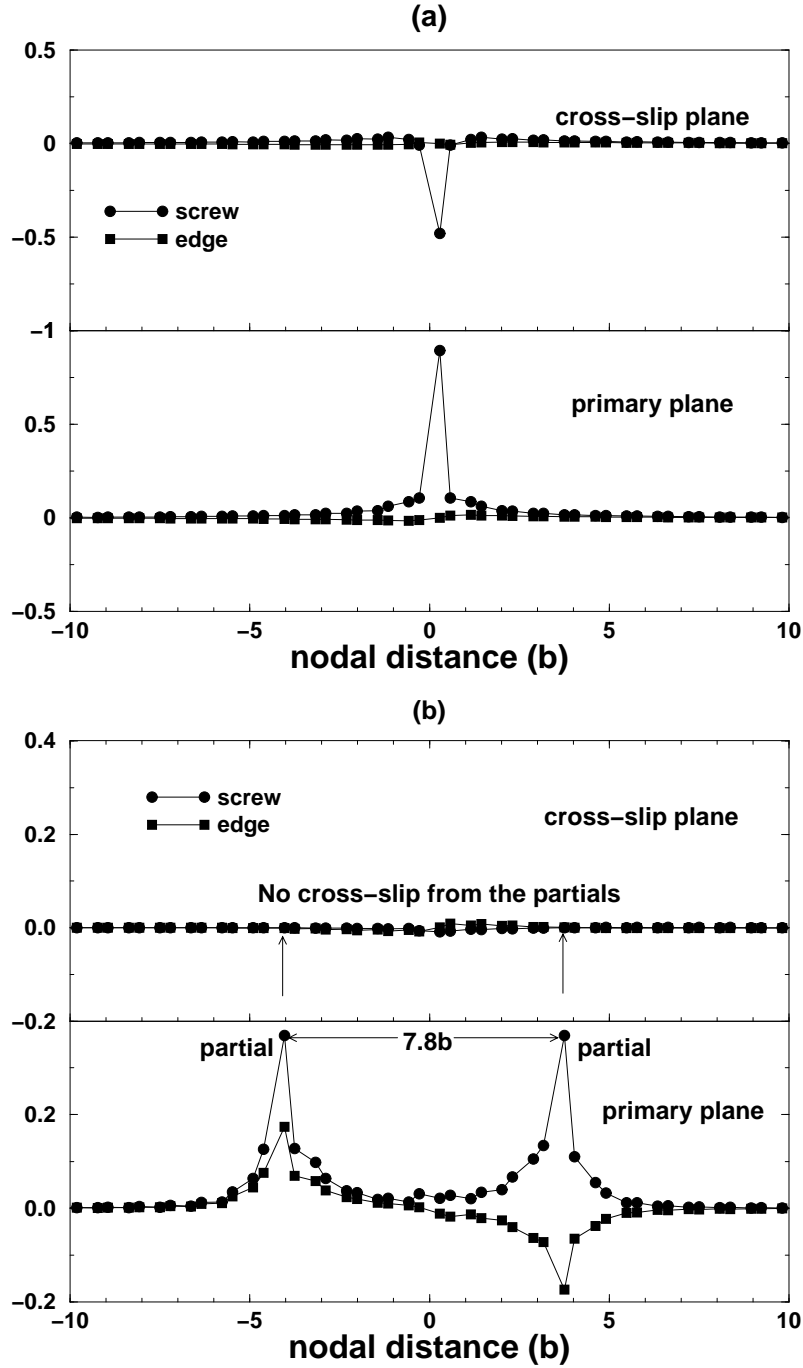


FIG. 3: Dislocation displacement density $\rho(x)$ for Al (Fig. 3(a)) and Ag (Fig. 3(b)). The peaks in the density plot in Fig. 3(b) represent partial dislocations.

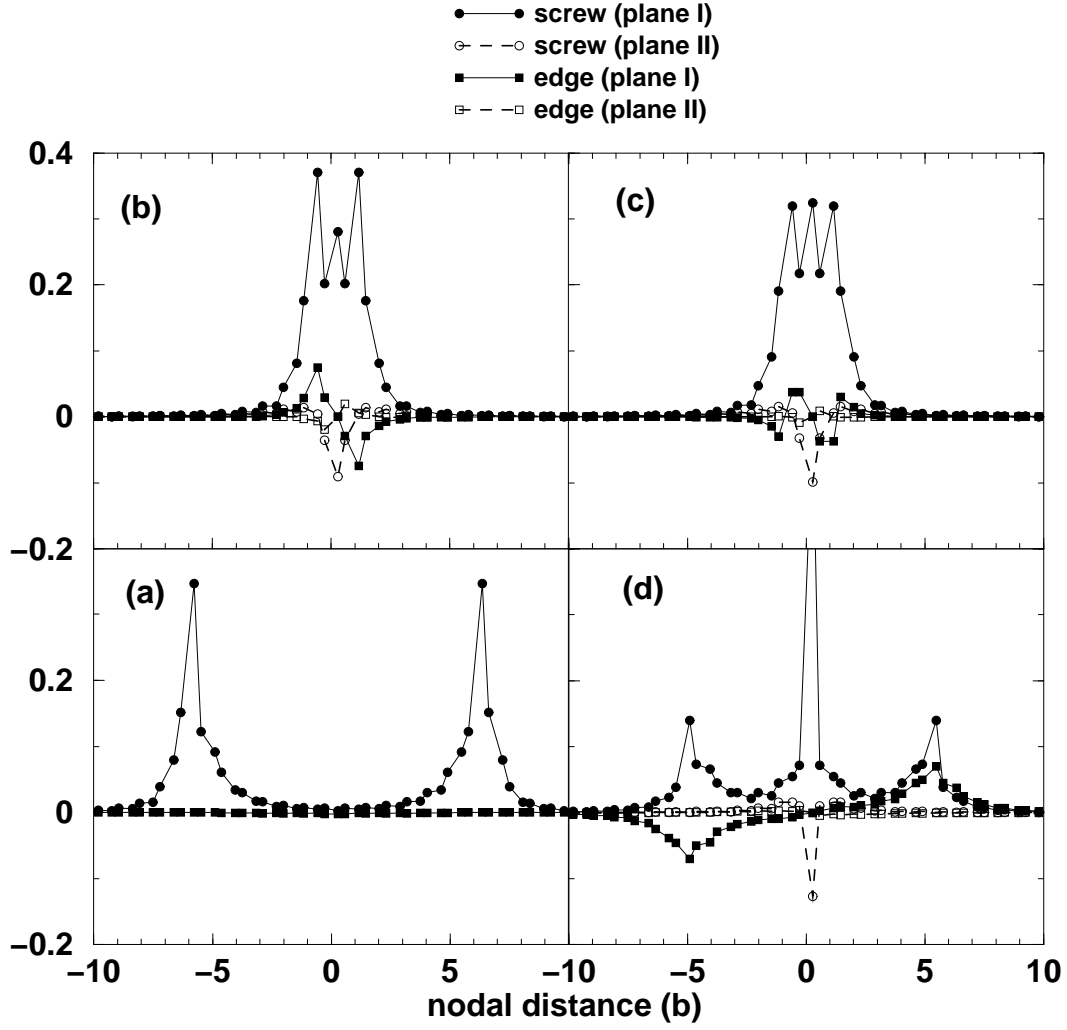


FIG. 4: Displacement density $\rho(x)$ for the screw dislocation in Ag under different Escaig stress. The solid (dashed) line and closed (open) symbols represent the dislocation density at the primary (cross-slip) plane. The screw and edge components of $\rho(x)$ are represented by circle and square, respectively. The external Escaig stress is (a) $\tau_1^I = 0.32$ GPa, (b) $\tau_1^I = -0.48$ GPa, (c) $\tau_1^I = -0.64$ GPa, and (d) $\tau_1^I = -3.2$ GPa, respectively.

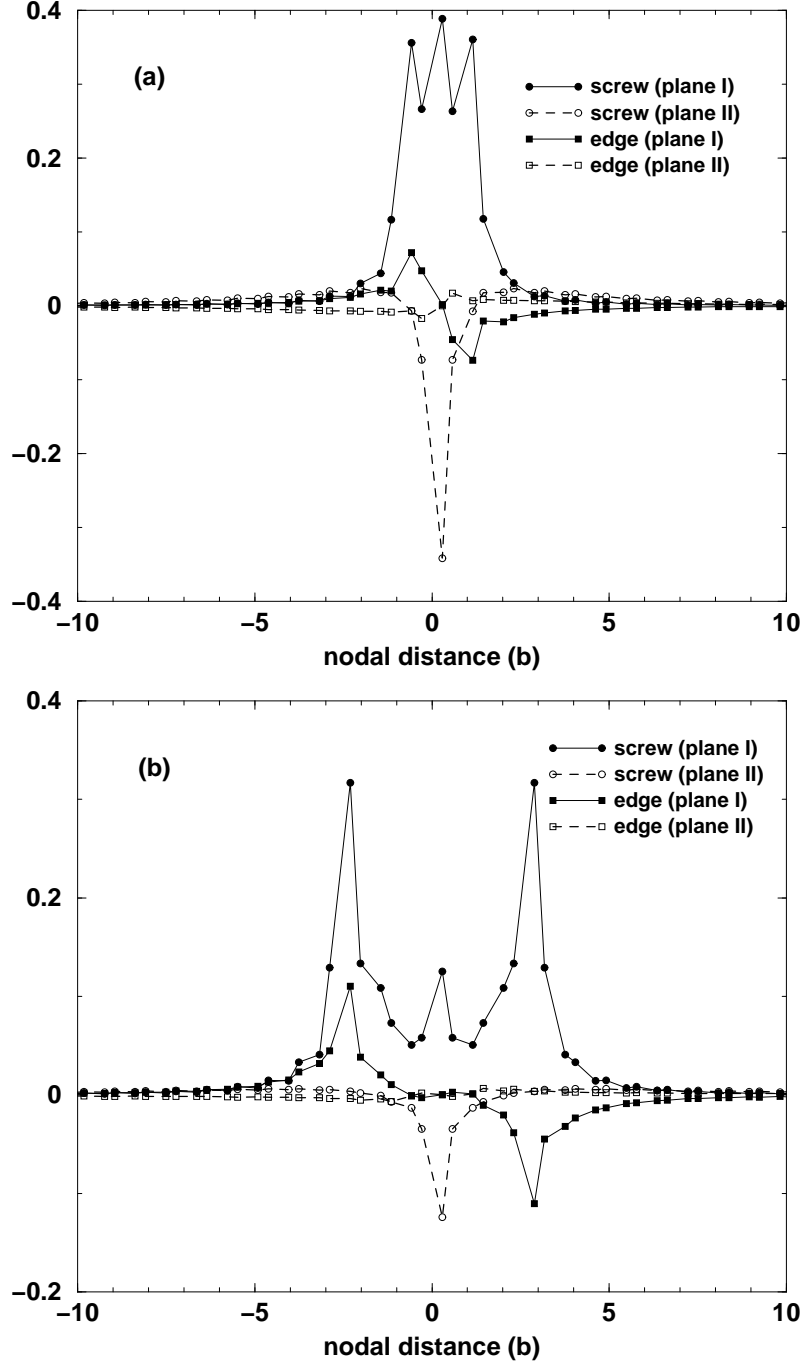


FIG. 5: Displacement density $\rho(x)$ for the screw dislocation in Al under different Escaig stress. The solid (dashed) line and closed (open) symbols represent the dislocation density at the primary (cross-slip) plane. The circle and square represent the screw and edge components of $\rho(x)$, respectively. The external Escaig stress is (a) $\tau_1^I = 0.96$ GPa and (b) $\tau_1^I = 1.92$ GPa, respectively.